Optical memory effect in square multimode fibers

Antonio Caravaca-Aguirre, Adrien Carron, Sylvain Mezil, Irène Wang, Emmanuel Bossy

Optical memory effect in square multimode fibers

ANTONIO M. CARAVACA-AGUIRRE[1], ADRIEN CARRON[1], SYLVAIN MEZIL[1], IRÈNE WANG[1], AND EMMANUEL BOSSY[1,*]

[1] *Univ. Grenoble Alpes, CNRS, LIPhy, F-38000 Grenoble, France*
[*] *Corresponding author: emmanuel.bossy@univ-grenoble-alpes.fr*

Compiled November 25, 2022

We demonstrate experimentally the existence of a translational optical memory effect in square-core multimode fibers. We found that symmetry properties of square-core waveguides lead to speckle patterns shifting along four directions at the output for a any given shift direction at the input. A simple theoretical model based on a perfectly reflective square waveguide is introduced to predict and interpret this phenomenon. We report experimental results obtained with 532-nm coherent light propagating through a square-core step-index multimode fiber, demonstrating that this translational memory effect can be observed for shift distances up to typically 10 microns after propagation through several centimeters of fiber.

http://dx.doi.org/10.1364/ao.XX.XXXXXX

The so-called memory effect has attracted considerable attention since the seminal work by Feng and Freund in the 80s [**?** **?**]. In the optics community, the optical memory effect refers to the fact that the wavefront transmitted or reflected by a scattering material will tilt or shift, but otherwise not change, when the incident wavefront is tilted of shifted [**?** **?** **?** **?**]. Beyond its interest for fundamental physics, as a particular class of input-output correlations, the optical memory effect have proven extremely useful to perform imaging through multiple scattering media, either by enabling calibration-free imaging methods [**?** **?**] or by extending the range of isoplanatic patches in wavefront shaping experiments [**?** **?**].

Highly multimode waveguides behave in many ways similarly to multiple scattering media, and many imaging methods developed to see through multiple scattering media have been adapted to perform imaging through multimode waveguides, most specifically through multimode fibers (MMFs) [**?** **?**]. Input-output correlation through MMFs in the form of some optical memory effect would thus enable the development of calibration free imaging methods inspired from those developed for scattering media [**?** **?**], which would revolutionize minimally invasive lensless microendoscopy. However, as opposed to thin scattering, it is generally acknowledged that there is no or limited memory effect in MMFs. Multicore fibers do exhibit a strong memory effect that can be exploited for lensless endoscopic imaging [**?** **?**], but involve propagation in bundles of single mode fibers, with a much larger footprint than MMFs with a comparable number of modes. In 2015, a rotational memory effect was reported for circular MMFs [**?**]. More recently, this rotational memory effect has further been combined with wavefront shaping to control and scan an optimized focus to achieve guided-star assisted imaging [**?**]. However, a 2D memory effect, required to perform calibration free imaging has to date never been reported with MMFs.

In this letter, we demonstrate the existence of a translational (shift-shift) memory effect in square-core MMFs. Although there has been pioneer research back in the seventies on imaging through square-core fibers [**?** **?**], square core MMF remain mostly unexplored for lensless endoscopic applications. Recently, Velsink *et al.* investigated square-core optical MMFs in the context of imaging and emphasize their scrambling properties and concluded on the absence of input-output correlations [**?**]. In our work, we show for the first time that despite their better scrambling property, square MMFs do actually exhibit input-output correlations in the form of a translational memory effect.

We first introduce a simple theoretical model of scalar wave propagation inside a perfectly reflective square waveguide, in order to provide simple physical insights on the translational correlations that we demonstrate experimentally in square MMFs. We consider a square waveguide of dimension d consisting of four perpendicular perfectly reflective mirrors (see Fig. 1 and its animated version as Supplementary information), and we assume a monochromatic scalar wave model. Here, "perfectly reflective mirrors" stands for interfaces with a reflection coefficient $r = \pm 1$ for all possible incidence angles. Wave propagation through a perfectly reflecting waveguide from some input plane ($z = z_a$) to some output plane ($z = z_b$) may be easily predicted with an image theory approach: as illustrated in Fig. 1, any input field $E_{\text{in}}(\mathbf{r}_a)$ defined inside the square waveguide of edge size d is indeed equivalent by image theory to an infinite periodic input field in free space of period $2d$ along the two transverse axis of the waveguide. If we now consider a shifted version of the input field $E_{\text{in}}(\mathbf{r}_a; \Delta\mathbf{r}_a) = E_{\text{in}}(\mathbf{r}_a - \Delta\mathbf{r}_a)$, with $\Delta\mathbf{r}_a = (\Delta x_a, \Delta y_a)$, Fig. 1 illustrates that the four different types of mirror images define four *periodic* input patterns in free space, which each shifts in one of the four directions defined by $\Delta\mathbf{r}_a^+ = +\Delta\mathbf{r}_a$, $\Delta\mathbf{r}_a^{\mp} = (-\Delta x_a, \Delta y_a)$, $\Delta\mathbf{r}_a^- = -\Delta\mathbf{r}_a$ and $\Delta\mathbf{r}_a^{\pm} = (\Delta x_a, -\Delta y_a)$. As a consequence from shift-invariant propagation in free space, the output field corresponding to the shifted version $E_{\text{in}}(\mathbf{r}_a - \Delta\mathbf{r}_a)$ of the input field may thus also be expressed as the sum of four output patterns that each shifts in one of the four directions

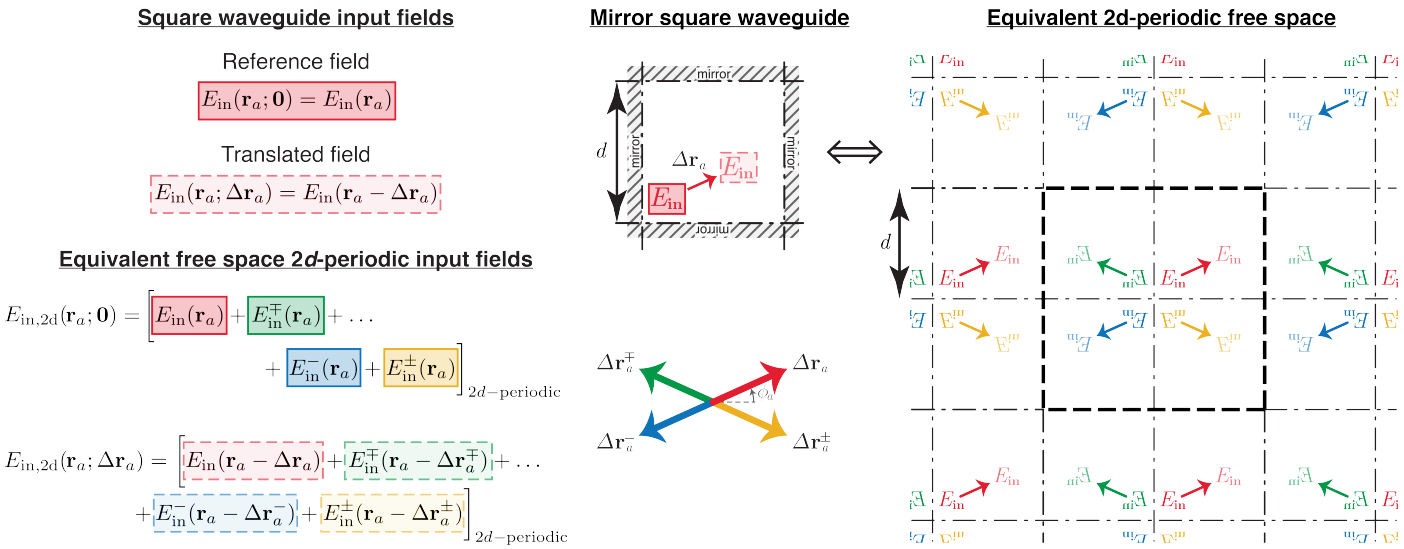

Fig. 1. Translational properties associated to a perfectly reflective square waveguide of dimension d. Based on image theory, an input field $E_{\rm in}(\mathbf{r}_a)$ defined inside the square waveguide is equivalent to a $2d$-periodic input field $E_{\rm in,2d}(\mathbf{r}_a)$ defined in *free* space. This $2d$-periodic input field consists of four $2d$-periodic sub-fields that each undergoes a shift when $E_{\rm in}(\mathbf{r}_a)$ undergoes a shift $\Delta\mathbf{r}_a$ (see also the animated illustration as Supplementary Information). The shift direction of each sub-field is given by one of the four possible images of $\Delta\mathbf{r}_a$ after mirror reflection on the boundary of the waveguide, noted $\Delta\mathbf{r}^{+}_a = \Delta\mathbf{r}_a$, $\Delta\mathbf{r}^{\mp}_a$, $\Delta\mathbf{r}^{-}_a$ and $\Delta\mathbf{r}^{\pm}_a$. As a consequence, the corresponding field at the output $E_{\rm out}(\mathbf{r}_b)$ may also be described as composed of four $2d$-periodic fields with the same translational properties, as further described in the Supplementary Information.

.

defined above. The explicit expressions of the output field and its four shifting components are provided in the Supplementary information. The corresponding total intensity pattern at the output plane may be derived from the field amplitude as

$$I_{\rm out,2d}(\mathbf{r}_b;\Delta\mathbf{r}_a) = I^{+}_{\rm out,2d}(\mathbf{r}_b-\Delta\mathbf{r}_a) + I^{\mp}_{\rm out,2d}(\mathbf{r}_b-\Delta\mathbf{r}^{\mp}_a) + I^{-}_{\rm out,2d}(\mathbf{r}_b-\Delta\mathbf{r}^{-}_a) + I^{\pm}_{\rm out,2d}(\mathbf{r}_b-\Delta\mathbf{r}^{\pm}_a) + I_{\rm out,interf,2d}(\mathbf{r}_b;\Delta\mathbf{r}_a) \quad (1)$$

Eq. 1 indicates that the intensity pattern corresponding to the shift of any input field can thus be described as four shifting intensity patterns on top of a non-shifting intensity pattern (resulting from cross-terms interference), and defines the translational optical memory effect considered in this work. While Eq. 1 is valid for any type of input and output fields, we focus in this work on output fields that can be described in first approximation by statistically uniform speckle fields, which are naturally formed by propagation through multimode fibers for mostly any input field. Under the assumption that the output intensity can be described as a second-order stationary speckle pattern, the normalized cross-correlation between two output intensity patterns corresponding to two shifted versions of a given input field may be defined as:

$$C(\Delta\mathbf{r}_b;\Delta\mathbf{r}_a) = \frac{\left\langle \delta I_{\rm out,k}(\mathbf{r}_b+\Delta\mathbf{r}_b;\mathbf{r}_{a_0}+\Delta\mathbf{r}_a)\times\delta I_{\rm out,k}(\mathbf{r}_b;\mathbf{r}_{a_0})\right\rangle_k}{\sqrt{\left\langle \delta I^2_{\rm out,k}(\mathbf{r}_b;\mathbf{r}_{a_0}+\Delta\mathbf{r}_a)\right\rangle_k}\times\sqrt{\left\langle \delta I^2_{\rm out,k}(\mathbf{r}_b;\mathbf{r}_{a_0})\right\rangle_k}} \quad (2)$$

The propagation through a multimode fiber being deterministic, an ensemble of input fields is required to produce an ensemble of random output fields. In Eq. 2, $\langle . \rangle_k$ refers to ensemble averaging of various realizations of statistically equivalent random input field, and $\delta I_{\rm out,k} = I_{\rm out,k} - \langle I_{\rm out,k}\rangle_k$ measures the fluctuations of the intensity fields.By further assuming that the four output fields can be described as four coherent *independent* complex gaussian speckle fields, $C(\Delta\mathbf{r}_b;\Delta\mathbf{r}_a)$ may be expressed analytically as

$$C_{\rm analytical}(\Delta\mathbf{r}_b;\Delta\mathbf{r}_a) = \frac{1}{16}\left|\sum_{\epsilon=\{+,\mp,-,\pm\}}\mu\left(2\pi\frac{\rm NA}{\lambda}||\Delta\mathbf{r}_b-\Delta\mathbf{r}^{\epsilon}_a||\right)\right|^2 \quad (3)$$

where $\mu(\theta) = \frac{2J_1(\theta)}{\theta}$ is the classical Airy pattern that describes the autocorrelation of a single speckle field amplitude, and NA is the numerical aperture. Predictions from Eq. **??** are plotted in Fig. 2, on which the four translating components of the total intensity patterns appear as four cross-correlation peaks. In the Supplementary information, we provide numerical computations with the *exact* fields propagated through our model waveguide, which confirm that Eq. **??** based on the assumption of independent speckle fields fully predicts the positions and amplitudes of the correlation peaks of interest. We note that for the special situation where $\Delta\mathbf{r}_a$ is parallel to one of the fiber axis, $\phi = 0°$ for instance, one gets $\Delta\mathbf{r}^{+}_a = \Delta\mathbf{r}^{\pm}_a$ and $\Delta\mathbf{r}^{-}_a = \Delta\mathbf{r}^{\mp}_a$, leading to two pairs of constructively interfering correlation peaks. As a consequence, the correlation amplitude corresponding to each pair of peaks is $1/4 = 25\,\%$ in this situation. In all other situations, the peak amplitude converges towards $1/16 = 6.25\,\%$. In summary, our idealized theoretical model predicts and explains the existence of a translational memory effect in the form of four shifting component at the output of square waveguides, and will now serve as a reference case to analyze our experimental results.

The existence of the optical memory effect introduced theoretically above was experimentally investigated using a step index optical fiber with a square core (CeramOptec, 100 μm × 100 μm core, NA= 0.22, length $L_{\rm fiber}$ = 3 cm). The experimental setup is

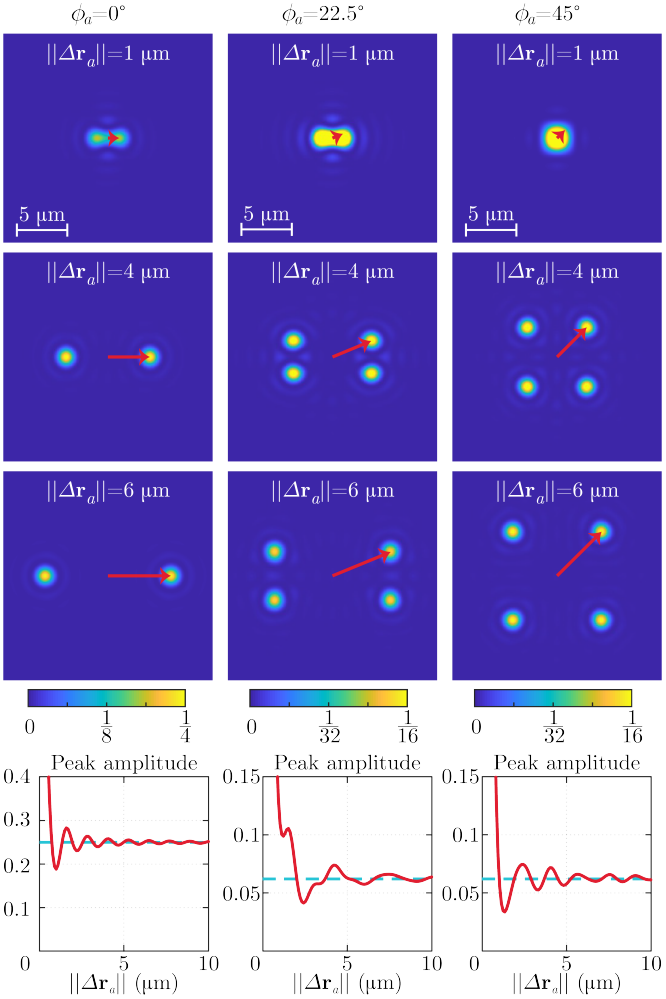

Fig. 2. Theoretical predictions for the correlation of output intensity patterns through a square waveguide for various shifts $\Delta\mathbf{r}_a$ of the input pattern. Images: $C_{\text{analytical}}(\Delta\mathbf{r}_b, \Delta\mathbf{r}_a)$ as a function of $\Delta\mathbf{r}_b$ for three values $||\Delta\mathbf{r}_a|| = 1\ \mu m$, $||\Delta\mathbf{r}_a|| = 4\ \mu m$, $||\Delta\mathbf{r}_a|| = 6\ \mu m$ and three directions $\phi_a = 0°$, $\phi_a = 22°$, $\phi_a = 45°$; $\Delta\mathbf{r}_a$ are depicted by red arrows. Curves: amplitude of $C_{\text{analytical}}(\Delta\mathbf{r}_a, \Delta\mathbf{r}_a)$ at the expected location of the (+) peak. The blue dashed line on the graphs represents the limit value for each case, 1/4 for $\phi_a = 0°$, 1/16 for $\phi_a = 22°$ and $\phi_a = 45°$.

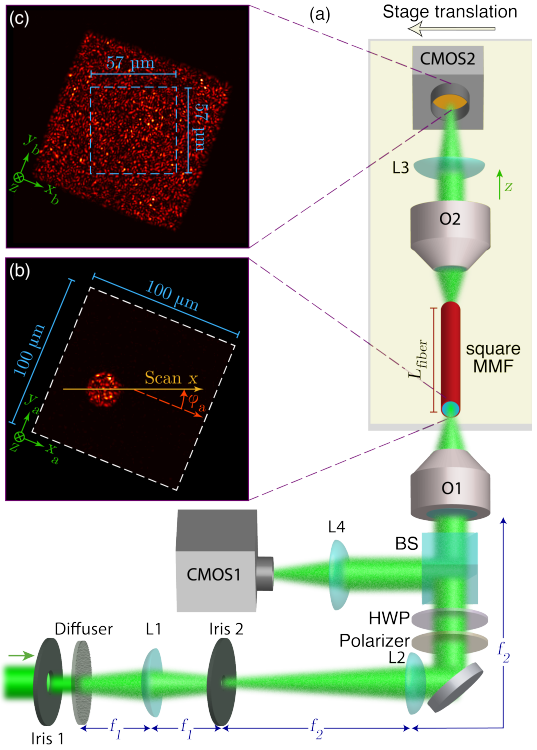

Fig. 3. (a) Experimental setup (further detailed in the Supplementary information). A coherent 532 nm beam is sent though a diffuser to create a speckled circular spot at the square fiber input. The MMF square fiber ($L_{\text{fiber}} = 3$ cm) and all following elements are held on a motorized translation stage to translate the input field relatively to the input facet. Cameras CMOS1 and CMOS2 respectively monitor the input (b) and output intensity patterns (c).

depicted on Fig. 3, and is further detailed in the Supplementary Information, along with movies showing the input and output patterns during a scan. The data processing method to derive cross-correlations $C_{\text{exp}}(\Delta\mathbf{r}_b; \Delta\mathbf{r}_a)$ from experimental data, in consistence with the theoretical expression 2 , is also detailed in the Supplementary Information. All the cross-correlation were computed from measurements inside a fixed square region of interest (ROI), as illustrated on Fig. 3.c.

Fig. 4 shows the cross-correlations $C_{\text{exp}}(\Delta\mathbf{r}_b; \Delta\mathbf{r}_a)$ obtained from the measured output intensity patterns, for various values of the translation distances $\|\Delta\mathbf{r}_a\|$ (1, 4 and 6 μm) and directions ϕ_a (0°, 22.5° and 45°). Importantly, these results correspond to $C_{\text{exp}}(\Delta\mathbf{r}_b, \Delta\mathbf{r}_a)$ computed from a *single* realization of the input speckle spot (see Fig. 3.b and section I.B of Supplementary Information). As the major result of our work, the cross-correlations obtained from the measured output speckle intensity patterns exhibit four peaks translating away from the center as the input shift increases, following the predictions from our idealized model. In the particular case ϕ_a=0°, only two peaks of much stronger amplitude are visible, in agreement with the theoretical predictions. To compare more quantitatively the experimental results to the theoretical predictions, the amplitude and position of each correlation peak as a function of input shift were measured via a tracking approach, and are reported in Fig. 5. For short translation distances, but large enough such that the correlation peaks can be resolved ($\|\Delta\mathbf{r}_a\| \gtrsim 1\ \mu$m), the measured peak amplitudes are on the same order as that predicted by the model. The positions of the four peaks are exactly those predicted from the theory, within the accuracy of the position tracking method. The oscillations resulting from the interference between the correlation peaks predicted by the theory for small shifts are also observed experimentally.

While the positions of the correlation peaks are exactly those predicted by our simple model, their amplitude decays and vanishes into the background for shifts on the order of 10 μm (see also movies as Supplementary Information), indicating that the observed translational memory effect has a limited range. A number of reasons may explain this limited range, which include the nature of the boundary conditions at the core cladding interface (different from that of a perfect mirror) and potential fiber geometrical imperfection (fiber twist, fiber bending, rounded corners) as compared to the idealized square geome-

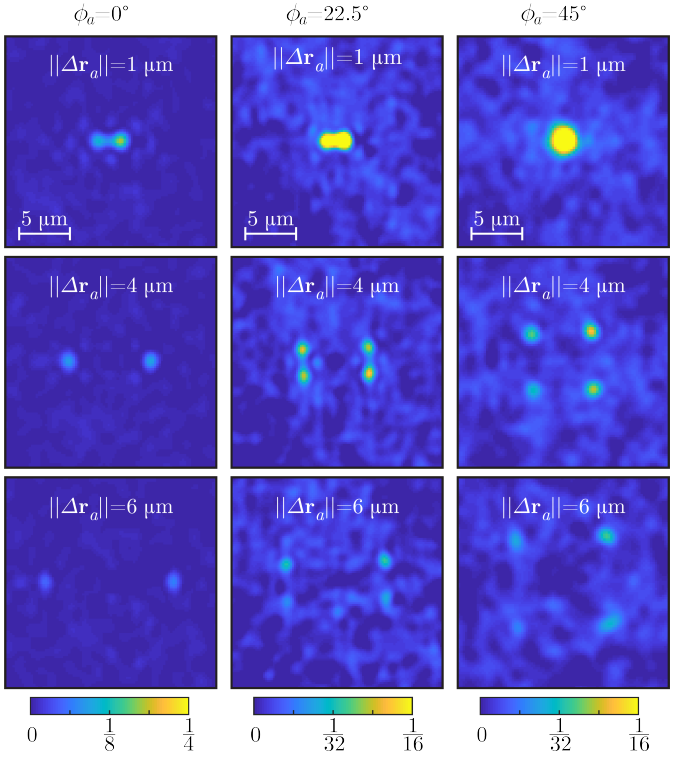

Fig. 4. Experimental results. Cross-correlations of the speckle patterns measured at the output of a 3 cm-long step-index square-core multimode fiber, obtained for various translation distances $\|\Delta\mathbf{r}_a\|$ (1, 4 and 6 μm) and directions ϕ_a (0°, 22.5° and 45°) of *one given* input pattern.

.

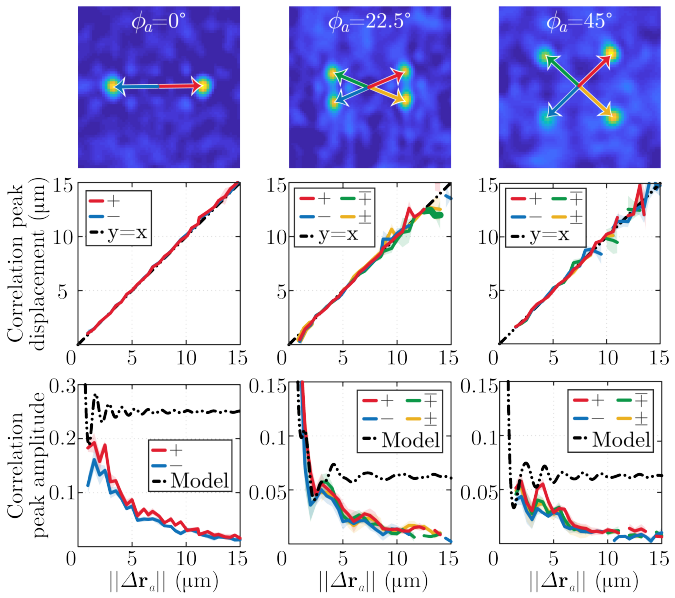

Fig. 5. Experimental results. Graphs: displacement and amplitude of the correlation peaks as a function of the input shift $\|\Delta\mathbf{r}_a\|$, for three translation direction ϕ_a (0°, 22.5° and 45°). The images correspond to experimental cross-correlations obtained for $\|\Delta\mathbf{r}_a\| = 4$ μm.

.

try. The purpose of our idealized model was limited to provide some physical understanding of the observed effect, as well as to provide upper bounds on the amplitude of the correlation peaks. Further investigations are required to explain and predict theoretically the observed finite range, likely by taking into account more realistic boundary condition and light polarization beyond the simple scalar model considered here. All the results presented here involved a linear polarization parallel to an edge of the fiber core. However, we also obtained similar results with other directions of the linear polarization (such as parallel or perpendicular to the translation direction), indicating that the observed memory effect is not strongly influenced by the polarization. Very interestingly, preliminary experiments with different fiber lengths up to 20 cm, and with significant fiber twists, indicate that the effect is robust, with a rather constant range for the memory effect.

In conclusion, we demonstrated experimentally the existence of a translational (shift-shift) memory effect in square multimode fibers, and proposed a simple idealized model that predicts and explains the origin of the observed effect. Much like the classical memory effect has been exploited to perform calibration-free imaging through a scattering medium, we envision that this new type of input-output correlation will be exploited for calibration-free imaging through square multimode fibers. While our experimental demonstration was performed here in optics in the visible range, our theoretical predictions are limited neither to this range nor to the field of optics, but are expected to apply to a wider range of situations including radio-frequency electromagnetic waves and acoustic waves in square waveguides.

Acknowledgements. ERC COHERENCE grant 681514. H2020 DARWIN grant 750420. The authors thank Dr. Dorian Bouchet for insightful discussions.

Disclosure. The authors declare no conflicts of interest.